Supplemental Material
for *Contact and Momentum Distribution of the Unitary Fermi Gas*

R. Rossi, T. Ohgoe, E. Kozik, N. Prokof'ev, B. Svistunov, K. Van Houcke, and F. Werner

(Dated: June 8, 2018)

We employ the resummation procedure of Ref. [1]: In order to resum a divergent diagrammatic series $\sum_N a_N$ for a quantity Q, we first construct a function $Q(z)$ whose Taylor series is $\sum_N a_N z^N$ and such that $Q(z=1)$ is the exact physical result. Taking into account the large-order behavior (to leading order, $|a_N| \sim (N!)^{1/5}$), we then take a generalized Borel transform $B(z)$, from which $Q(1)$ is retrieved by the inverse Borel transform $Q(1) = \int_0^\infty dt\, t^4\, e^{-t^5 - bt^4 - ct^3}\, B(t)$ (b being chosen as in Ref. [1]). The latter integral is evaluated using a conformal mapping taking into account the analytic properties of $Q(z)$ in the complex-z plane.

In the moderately degenerate regime, we have cross-checked the bold scheme with the ladder scheme, see Fig. S1. In the strongly degenerate regime, the ladder scheme is not applicable, but we have cross-checked different variants of the bold scheme, see Fig. S2, where we show three choices: $Q(z) = \Sigma(z)/z$ resp. $\Pi(z)/z$ with $c = 13$ (circles), the same $Q(z)$ with $c = 60$ (diamonds), and $Q(z) = \Sigma(z)$ resp. $\Pi(z)$ with $c = 60$ (squares). The error bars shown at each $N_{\max}$ take into account the statistical error due to the Monte Carlo process, as well as the error due to the finite number of iterations in the bold case.

In our final results, the error bars also include the estimated systematic errors due to the finite $N_{\max}$ as well as the grids used in the numerics, so that all sources of errors are taken into account. We provide our data for the contact in Table S1, and for the momentum distribution in the ancillary files `nk_betamu*.txt` for several $\beta\mu$ values.

We used the ladder scheme for $\beta\mu = -1$ and -0.5, and the bold scheme for all other $\beta\mu$ values. Our final results for the ladder-scheme cross-check at $\beta\mu = 0$ are $\mathcal{C}\lambda^4 = 30.32(15)$ and $\mathcal{C}/k_F^4 = 0.0800(3)$.

We went up to diagram order $N_{\max} = 10$ for $\beta\mu \le -1$, $N_{\max} = 8$ for $\beta\mu = 1.5$, and $N_{\max} = 9$ for all other $\beta\mu$ values. For the ladder scheme, we used $Q(z) = \mathcal{C}(z)$, with $c = 12$ for $\beta\mu = -1$, and $c = 10$ for $\beta\mu \in \{-0.5, 0\}$. For the bold scheme, we used $Q(z) = \Sigma(z)/z$ resp. $\Pi(z)/z$, with $c = 10$ for $0 \le \beta\mu \le 1$, $c = 15$ for $\beta\mu = 1.5$, $c = 13$ for $\beta\mu = 2$, and $c = 12$ for all other cases.

For an accurate comparison with the virial expansion, we show in Fig. S3, as a function of the fugacity $\zeta = e^{\beta\mu}$, the apparent third-order virial coefficient $c_{3,\mathrm{app}}(\zeta) := (\mathcal{C} - \mathcal{C}_{\mathrm{virial}\,2})\lambda^4/(16\pi^2\zeta^3)$. By construction, $c_{3,\mathrm{app}}(\zeta) \to c_3$ in the non-degenerate limit $\zeta \to 0$. Our data for $c_{3,\mathrm{app}}(\zeta)$ do become fairly close to the accurate value of c_3 from [2, 3] but the slope of $c_{3,\mathrm{app}}(\zeta)$ has to change sign for $\zeta \lesssim 0.2$. The coefficient c_3 comes from the three-body propagator [2, 4] which has to be reconstructed in our framework by summing an infinite number of diagrams.

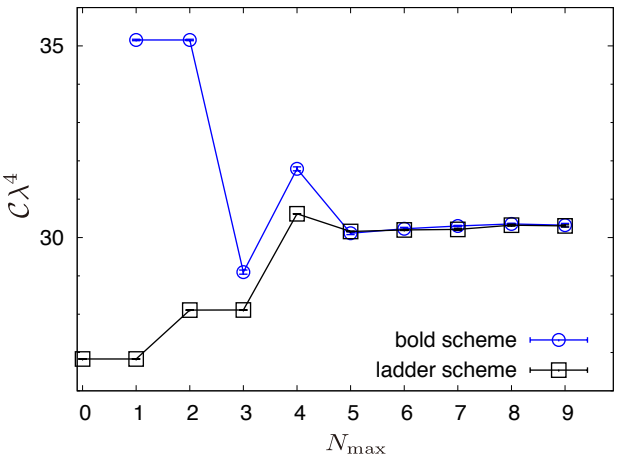

FIG. S1: Resummed dimensionless contact *vs.* maximal diagram order $N_{\max}$ at $\beta\mu = 0$ ($T/T_F \approx 0.6$). The two different diagrammatic schemes agree with each other in the large $N_{\max}$ limit.

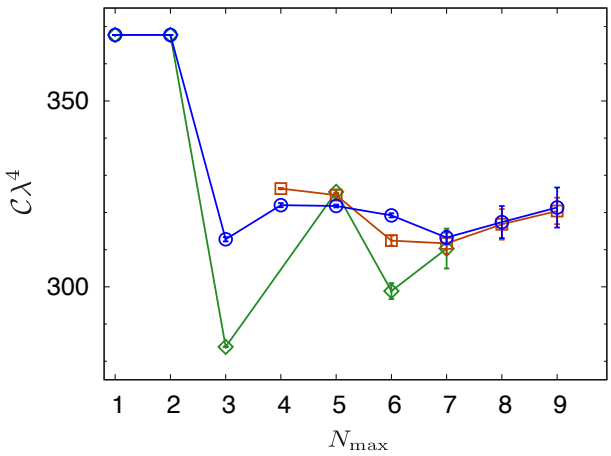

FIG. S2: Resummed dimensionless contact *vs.* maximal diagram order at $\beta\mu = 2$ ($T/T_F \approx 0.2$). Three different variants of the conformal-Borel transformation are used (see text).

$\beta\mu$	T/T_F	$\mathcal{C}\lambda^4$	$\mathcal{C}/k_F^4$
-1.5	1.9961(1)	2.248(2)	0.05671(4)
-1	1.3640(3)	5.661(15)	0.0667(2)
-0.5	0.9314(4)	13.59(3)	0.07470(9)
0	0.6449(4)	30.32(8)	0.0799(2)
0.5	0.4601(10)	62.0(6)	0.0831(6)
1	0.3415(12)	114.7(1.8)	0.0848(10)
1.5	0.2631(16)	198(5)	0.0869(15)
2	0.2103(11)	320(7)	0.0895(18)
2.25	0.1892(15)	396(12)	0.0898(18)

TABLE S1: The contact $\mathcal{C}$ as a function of temperature.

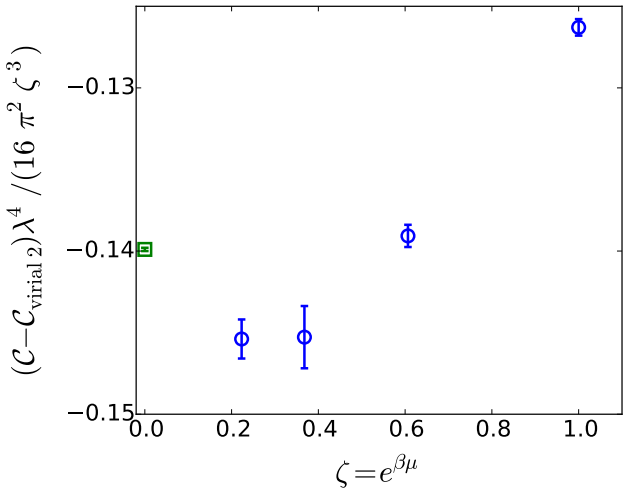

FIG. S3: Circles: Diagrammatic Monte Carlo data for the difference between the contact $\mathcal{C}$ and its 2nd order virial expansion $\mathcal{C}_{\text{virial 2}}$, divided by an appropriate factor. This quantity must tend to the virial coefficient c_3 from [2, 3] (square) in the zero fugacity limit $\zeta \to 0$.

[1] R. Rossi, T. Ohgoe, K. Van Houcke, and F. Werner, *Resummation of diagrammatic series with zero convergence radius for strongly correlated fermions*, arXiv:1802.07717.
[2] M. Sun and X. Leyronas, Phys. Rev. A **92**, 053611 (2015).
[3] X. Leyronas, *private communication.*
[4] X. Leyronas, Phys. Rev. A **84**, 053633 (2011).